Fully Three-Dimensional Tomographic Evolutionary Reconstruction in Nuclear Medicine

Aurélie Bousquet[1], Jean Louchet[1], Jean-Marie Rocchisani[1,2]
[1]INRIA Rocquencourt/ COMPLEX, Domaine de Voluceau, B.P. 105. 78153 Le Chesnay, France
[2] Paris XIII University, UFR SMBH & Avicenne hospital, 74 rue Marcel Cachin. 930013 Bobigny, France

aurelie.bousquet@inrets.fr, jean.louchet@inria.fr, jean-marie.rocchisani@{avc.aphp.fr, inria.fr}

Abstract. 3-D reconstruction in Nuclear Medicine imaging using complete Monte-Carlo simulation of trajectories usually requires high computing power. We are currently developing a Parisian Evolution Strategy in order to reduce the computing cost of reconstruction without degrading the quality of results. Our approach derives from the Fly algorithm which proved successful on real-time stereo image sequence processing. Flies are considered here as photon emitters. We developed the marginal fitness technique to calculate the fitness function, an approach usable in Parisian Evolution whenever each individual's fitness cannot be calculated independently of the rest of the population.

Keywords. Computer Tomography, Emission Tomography, Artificial Evolution, Parisian Evolution, FlyAlgorithm, Compton scattering, Nuclear Medicine

1. Introduction

1.1 Nuclear medicine

In Nuclear Medicine diagnosis, radioactive substances are administered to patients using a tracer molecule containing a radioactive marker. The distribution of radioactivity in the body is then estimated from the radiation detected by gamma cameras. In order to get an accurate estimation, a three-dimensional tomography is built from two-dimensional scintigraphic images..

Some artefacts due to scattering and absorption are then to be corrected. Existing analytical and statistical methods are costly and require heavy computing. The main variants of Nuclear Imaging are SPECT (Single Photon Emission Computed Tomography) and PET (Positon Emission Tomography). Radioactive tracers are photons or positons emitters. Compared to other tomography techniques as X-ray scanning or Magnetic Resonance Imaging, Nuclear Imaging brings useful information on biological and metabolic function. The marker most widely used in SPECT is Technetium 99m (99mTc), with a half-life of about 6 hours and emitting photons at an energy level of 140keV, which is well adapted to current gamma-camera technology. In planar mode, the gamma camera is fixed and collects a plain two-dimensional projection of the radioactive tracer concentration. In tomographic mode, the gamma camera rotates around the patient. A gamma camera can also be used in

static or dynamic mode, allowing to monitor how the radioactive tracer concentration evolves in the body. The main limitations of this technology are:

- sensor performance (resolution, sensitivity),
- physical effects (absorption, scattering, noise),
- motion of patient (long exposure times),
- accuracy of reconstruction algorithms.

1.2 The Compton effect and its consequences

Rayleigh effect occurs when a photon meets an atom without disturbing its electronic structure. The photon then gets deviated but keeps its original energy. With high energy photons, this effect is negligible except in the gamma camera crystal itself. In photoelectric interaction, our photon is completely absorbed by an atom which then emits a fluorescence photon to carry the excess energy. This is the basic process of photon detection in the gamma camera.

The Compton effect is by far the dominant perturbation during the transit of high energy photons from the tracer through the body. Both absorption and scattering induce important effects on image quality, as they vary with the nature and thickness of the part of the body involved. Compton scattering with important energy losses will have a larger than average deviation angle.

The photons with an energy level close to the initial level have a small probability of having been deviated. However, the energy resolution of gamma cameras is not sufficient to always ascertain whether a photon has been deviated or not. In order to correct attenuation, it is possible to use a X-ray CT scanner image which gives an accurate representation of the attenuation map in the body; however, a uniform attenuation map may be used when the organ is homogeneous enough. On the other hand, scattering is more difficult to deal with. The main algorithm families [1, 2, 7] are:

- subtraction algorithms using energy windows to filter primary electrons,
- deconvolution algorithms which consider scattering is a uniform process,
- recombination algorithms (based *e.g.* on principal component analysis).

Our long-term aim is to correct Compton scattering using Evolutionary Computation in order to get faster results with a level of quality similar to present high cost algorithms. The first step presented in this paper is the validation of an evolutionary 3-D reconstruction algorithm with a simplified propagation model, allowing future replacement of the propagation module with a more accurate model [6] including the modelling of Rayleigh and Compton effects. Contrary to standard reconstruction algorithms: Filtered back projection (FBP) and Ordered Subset Expectation Maximisation (OSEM) where the problem is split into parallel 2-D slices and not all sensor data are used, our method pertains to the family of "fully 3-D" reconstruction methods.

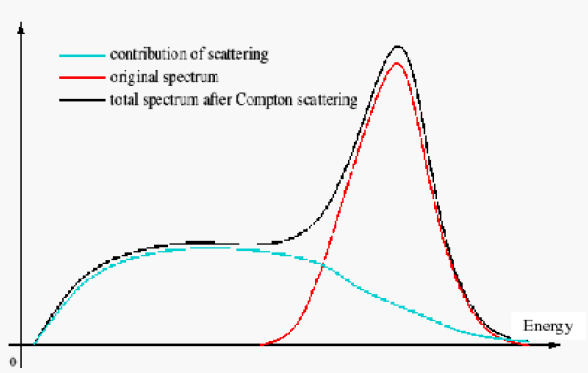

Fig. 1. Detection spectrum of gamma photons

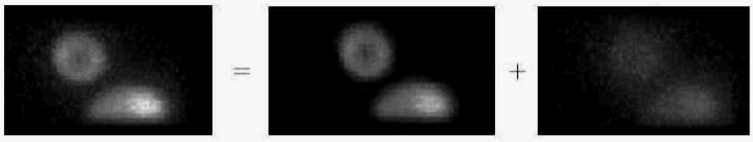

Fig. 2. Contributions of primary and scattered photons.

2. A Parisian Evolutionary Approach

2.1 The classical Fly algorithm

The original Fly Algorithm [5] is a 3-D evolutionary reconstruction method based on the Parisian Approach. Each individual ("fly") represents a point of space and the whole population of flies is the representation of the object detected. It uses a fitness function based on the consistency of grey level properties of the projections of the fly on the images taken by each camera. It has been first used on stereovision [4].
Here, the semantics of the fly is enriched as we will now consider the fly is a photon emitter. Again, the algorithm evolves a population of flies which eventually converge to the three dimensional shape to be detected. While this approach has been validated in its principles, computation costs were still high due to the complexity of physically modelling random photon trajectories, and the reconstruction results were not quite up to the vquality expected or obtained through more classical methods. Following this, we developed an innovative evaluation function based on a specific approach to fitness calculation, called "marginal fitness", giving encouraging results on both simplified synthetic data and real scintigraphic images.

2.2 Monte-Carlo simulation

Monte-Carlo simulation [3] is well adapted to nuclear medicine with its particle emission, propagation and detection random processes. Each photon trajectory is processed separately. The photon is propagated through space cells where it can be absorbed or scattered conforming to suitable random depending on the local environment. Each photon thus carries his own including which fly was its source. In a first approach, we considered the patient's body as a homogeneous cylinder. A later, more refined approach consists of using an absorption map in function of the material involved.

2.3 Building a fitness function

Radioactive tracers are only present in the central search zone, which contains the patient's body. The "screens" are the different positions of the gamma camera crystals. A fly is defined as a photon emitter and is described by its coordinates (x, y, z).

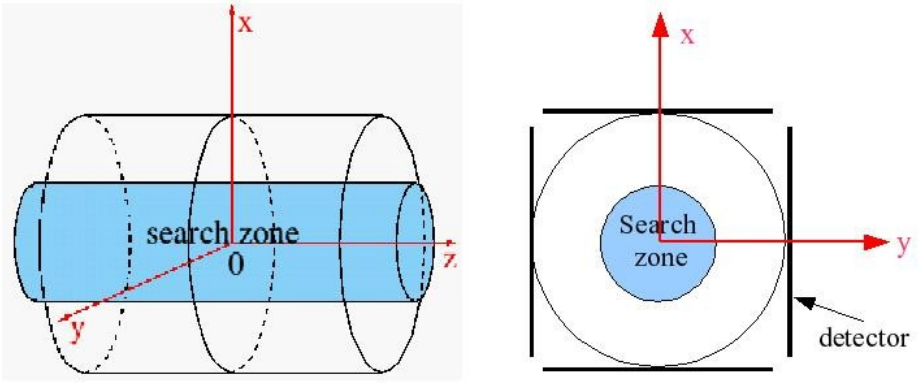

Fig. 3. Modeling the tomographic system: lateral view (left), axial view (rigth)

We first validated the principles of an evolutionary approach using a simplified, homogeneous model of the body, and a bonus-based fitness function: each simulated photon that reached a detector cell had a contribution to the fitness of its originator fly proportional to the actual number of photons received by this cell. The high number of Monte-Carlo simulations led to unrealistic processing time. In a second approach, in order to speed up processing, we defined a number of archetypal flies characterised by their distance from the detectors, while the search space was still considered homogeneous. Monte-Carlo simulation was performed on each archetypal fly and the results stored to be used as a lookup table in the evolutionary process. Evolution was then run calculating fitness values based on pre-calculated Monte-Carlo results, leading to less than half the original computation time. However this approach cannot take into account the heterogeneity of matter and it lacks precision, so that we had to concentrate on developing a fitness function that be fast, accurate and open to heterogeneity.

The overall process is summarized by the following diagram:

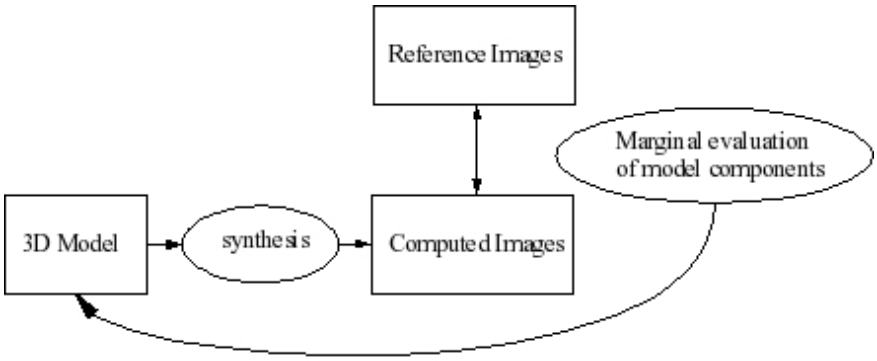

Fig. 4. The 3D Evolutionary reconstruction

Bonus fitness. While reducing the number of photons emitted by each fly to only 4 photons initially oriented orthogonally to the detectors gave a substantial improvement in calculation time, experience showed an important backside of bonus-based fitness: in presence of several bright objects, the flies will tend to accumulate on the brightest or biggest object at the expense of the other ones. This is illustrated on the following images: the 3-D scene consists of two cubes of different size and brightness; the image on the left shows what an ideal reconstruction algorithm should have given, and the right image what it actually gave using bonus fitness. The same behaviour was found on all similar data.

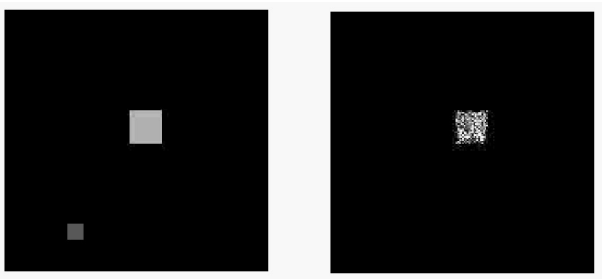

Fig. 5. Bonus fitness: loss of smaller objects (left: ideal image; right: actual reconstruction, side view).

Marginal fitness. Rather than evaluating a fly independently of its context, we introduced marginal evaluation by defining the fitness of a particular fly as its contribution (positive or negative) to the whole population's Fitness:

$$\text{fitness}(i) = \text{Fitness}(\text{population} - \{i\}) - \text{Fitness}(\text{population}) \quad (\mathbf{0})$$

To this end, the Fitness of a given population is given by the likeness of the projection images generated through Monte-Carlo simulation, with the actual images given by the sensors. As the grey level of the synthesised images depends on the number of

flies, a normalization factor must be introduced in order to compare the natural and synthetic projections.

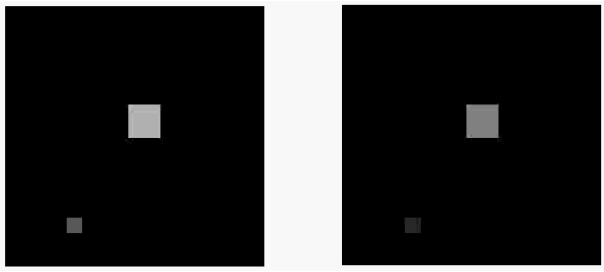

Fig. 6. Marginal fitness: better detection of smaller objects (left: ideal image; right: actual reconstruction), side view.

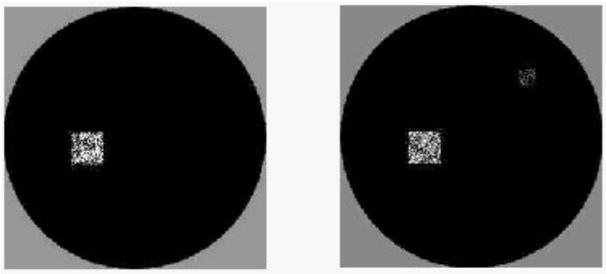

Fig. 7. Top views of results with bonus (left) and marginal (right) fitness functions

Rotating screens . Rotating screens are often used in SPECT imaging, with up to 128 screen positions. In order to exploit all the data while keeping memory requirements down, only 4 screens are used for fitness calculation and periodically rotated.

3. Results

The following results have been calculated from real SPECT images using the algorithm described above. In the current state of research, we did not include detailed Monte-Carlo simulation of absorption and Compton scattering into these experiments which only demonstrate the validity of the fly-based reconstruction algorithm. Integration of a fast Monte-Carlo simulation into the algorithm will be necessary to obtain high quality results.

3.1 Example 1

The objects are three cylinders with different brightness and diameter. The parameters are given in table 1.

Table 1. Parameters used in synthetic data reconstruction

projection image size	128*128
number of flies	266000
number of screens used at each generation	4
total number of screens	128
screens rotated every	5 generations
number of generations	1000
probability of mutation	50,00%
decrease of pm per generation	5,00%
probability of crossover	0,00%
mutation factor	1cm

As this is usual with Parisian Evolution, high mutation rates are used while crossover is not always essential to performance.

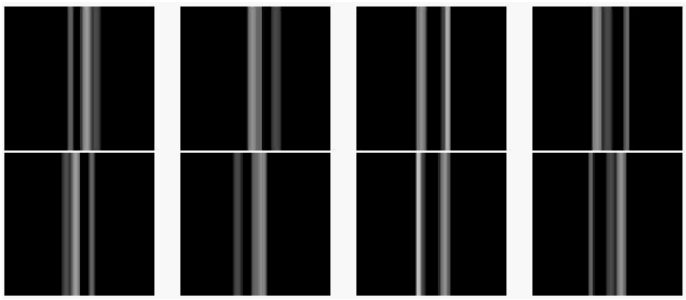

Fig. 8. Synthesised projections of the object, viewed under different angles: n / 4, n ∈ [0,7]}

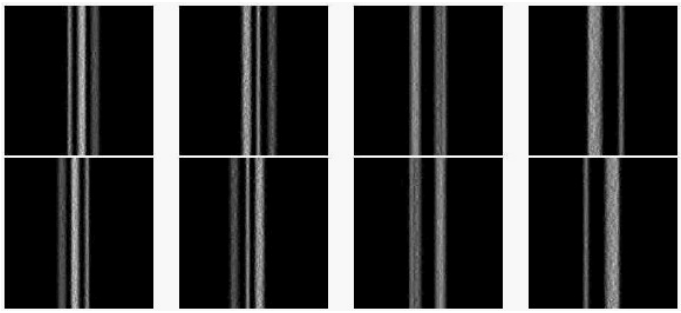

Fig. 9. Side views of the 3-D reconstructed object (flies) under the same angles

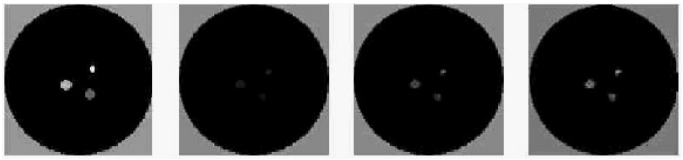

Fig. 10. Views of original object (left) and reconstructions (slices of 5, 10 and 20 pixels).

3.2 Example 2

Here, there are 3 nested objects with different brightness. The algorithm parameters are the same as in the previous example.

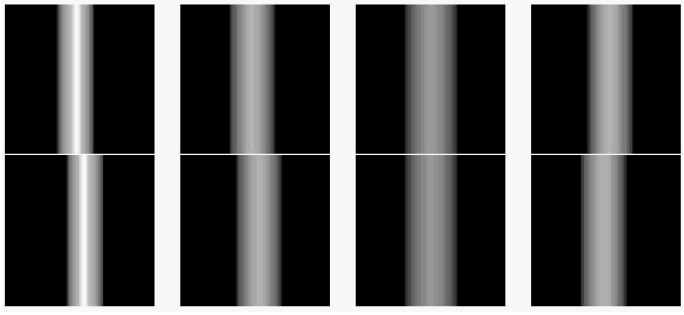

Fig. 11. Synthesised projections of the object, viewed under different angles.

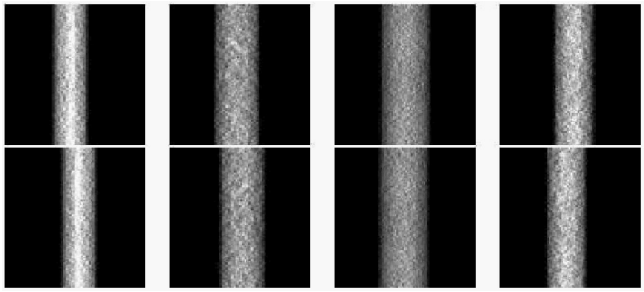

Fig. 12. Side views of the 3-D reconstructed object (flies) under the same angles.

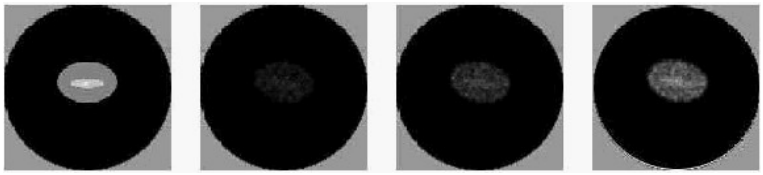

Fig. 13. Top views of the 3-D reconstructed object: original object (left) and its reconstructions (slices of 5, 10 and 20 pixels).

3.3 Example 3: real data

We tested the algorithm on actual images of bone scintigraphy, with the following parameters:

Table 2. Parameters used in bone scintigraphy reconstruction

projection image size	128*128
number of flies	1017500
number of screens used at each generation	4
total number of screens	64
screens rotated every	5 generations
number of generations	1000
probability of mutation	50,00%
decrease of pm per generation	5,00%
probability of crossover	0,00%
mutation factor	1cm

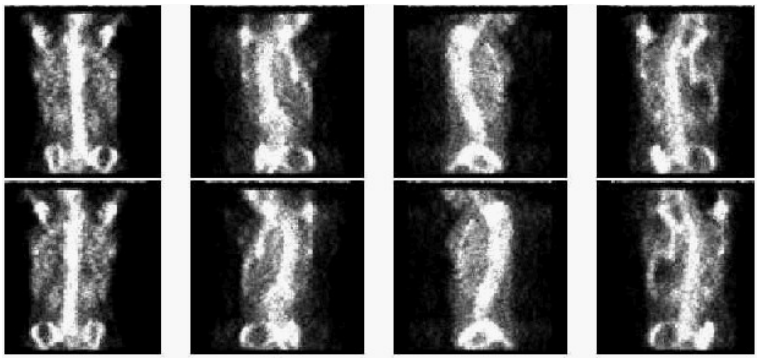

Fig. 14. Original projection acquired around the patient

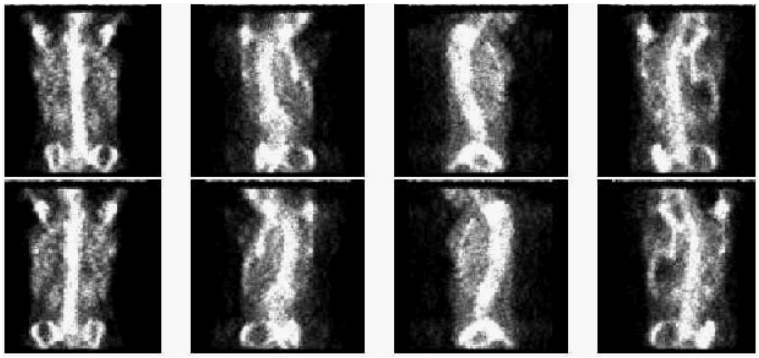

Fig. 15. Side views of the 3-D reconstructed object (flies).

Our algorithm was compared with a commercial 2D OSEM reconstruction. It well recovers shapes and contrast, with a processing time around 10 times longer than the optimized OSEM.

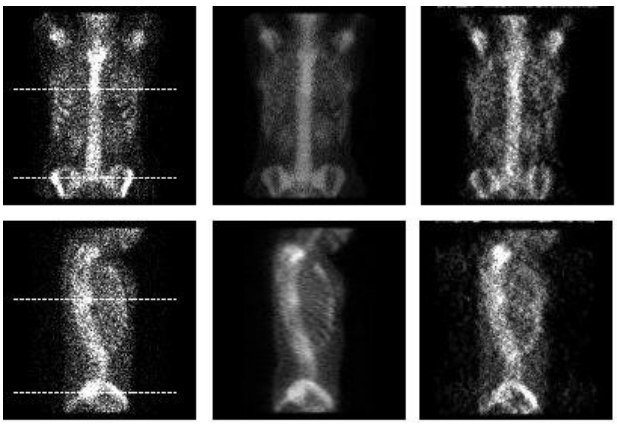

Fig. 16. Projections of the 3-D reconstructed object (flies): Acquisition (left), OSEM (middle), Flies (right).

Fig. 17. Axial views of the same 3-D reconstructed object (flies), at waist (upper row) and

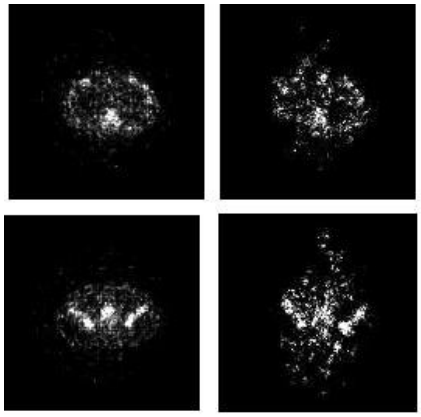

thorax (lower) levels. (Dash lines of figure 16). OSEM (left) and Flies (right) reconstructions.

3.4 Example 4: noise resistance

In this test example, a Gaussian noise has been added to the images of example 1 (Fig. 9) and the same algorithm parameters have been used.

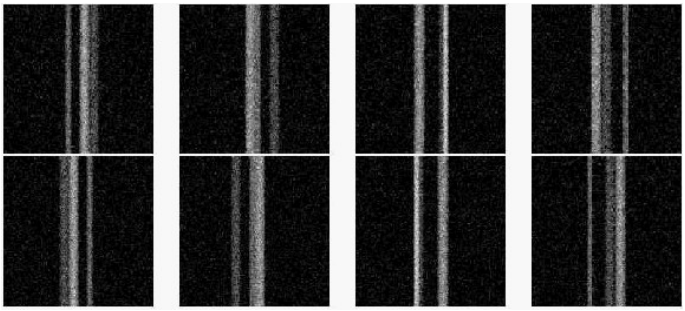

Fig. 18. Noisy synthesised projections of the object.

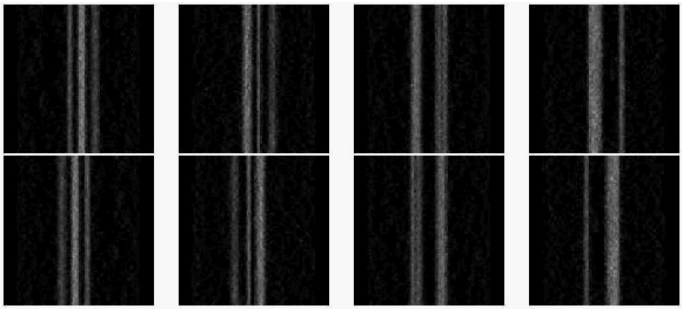

Fig. 19. Side views of the 3-D reconstructed object

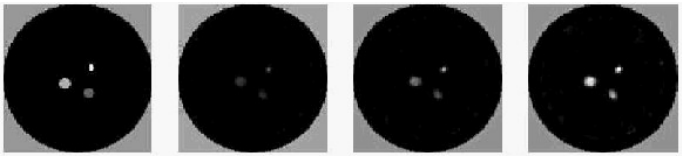

Fig. 20. Top views of the object reconstructed from noisy images (slices of 5, 10 and 20 pixels).

We observe that reconstruction is fairly noise resistant, probably thanks to the fact screen redundancy is exploited by the algorithm, although the brightness differences between the three cylinders are not rendered as clearly as with the noiseless images.

4 Conclusion

We demonstrated the validity of a generalization of the Fly algorithm introducing the marginal fitness calculation method, to constructing the 3-D shape of radioactive tracer concentration from SPECT images. Contrary to more classical approaches, our "fully 3-D reconstruction method" exploits all the projection images. The next stages of this research will concentrate upon building simplified but accurate models of scattering and absorption derived from complete Monte-Carlo simulation of Compton and Rayleigh scattering, exploit energy level information and x-ray absorption data, in order to get high quality results in realistic times. More elaborate validations than visual inspection must be achieved with ground truth images than only could be obtained by sophisticated Monte Carlo simulations.

Acknowledgements. We wish to specially thank the students who contributed to the ideas and methods presented in this paper and their implementation and testing, in particular: Sébastien Gaucher, Charles Brintet, Lionel Castillon, Marie Thépaut, Maria Rodriguez Lopez.

References

1. F. Bonnin, I. Buvat, H. Benali, R. di Paola Scatter correction in scintigraphy: the state of the art, European Journal of Nuclear Medicine, 21(7), July 1994.
2. M. Kalos, P. Wittlock, Monte-Carlo methods, John Wiley and Sons, 1986.
3. J. Louchet, Stereo Analysis Using Individual Evolution Strategy, ICPR2000, Barcelona, Spain, September 2000 .
4. J. Louchet, Model-based Image Analysis using Evolutionary Strategies, to appear in: Genetic and Evolutionary Computation in Image and Computer Vision, Cagnoni ed., Springer, 2007.
5. SIMSET ("Simulation System for Emission Tomography") software, University of Washington: http://depts.washington.edu/simset/html/simset_main.html
6. J. C. Yanch, M.A. Flower, S. Webb, A comparison of deconvolution and windowed subtraction techniques for scatter compensation, in SPECT, IEEE transactions on Medical Imaging, 7(1), March 1988.